Vol. 4 No. 4 ADVANCES IN ATMOSPHERIC SCIENCES November 1987

THE EFFECTS OF FRICTION AND HEATING OF CONVECTIVE CONDENSATION IN THE BAROCLINIC INSTABILITY PROBLEM

Zheng Weizhong (郑维忠) and *Yu Zhihao* (余志豪)

Department of Atmospheric Sciences, Nanjing University

Received January 10, 1986.

ABSTRACT

By using the β-plane, two-layer quasi-geostrophic baroclinic model, this paper discusses the baroclinic instability problem concerning the effects of friction and heating of convective condensation. By linear analysis it is shown that the combination of β effect, friction and convective heating brings about the asymmetric phenomenon of margin curves. The convective heating plays a role in the increased baroclinic instability. As the heating increases ($m^* \to 1$), the short wave cutoff can increase infinitely. Besides, the numerical integration of the finite-amplitude equations shows that the trajectory on the phase plane oscillates periodically in the case of non-dissipation. When the friction dissipation is considered, the trajectory of phase decays and oscillates to the equilibrium. The stronger convective heating not only makes the unstable wave length shorter and the amplitude of the equilibrium decrease, but also makes multiple equilibrium into single equilibrium.

I. INTRODUCTION

The baroclinic instability theory was first put forward by Jaw (1946), Charney (1947) and Eady (1949) et al. Recently, by using a simple f-plane, two-layer model, Pedlosky (1970, 1971, 1980, 1981) discussed the interaction between disturbance and basic flow and showed that the periodic, chaotic and steady behavior would appear in the baroclinic finite-amplitude wave of weak instability.

By using a β-plane, two-layer model, this paper introduces the effects of friction and heating of convective condensation on baroclinic instability. By introducing weak β effect (an order smaller than the relative vorticity gradient), Pedlosky (1981) found that the phenomena of chaos and period halvings would appear only in proper friction and small β, and would appear in steady solutions under stronger β effect. Besides, Ekman friction on the upper and lower boundaries makes the system become a dissipative one. Pedlosky (1983) studied the dynamic problem of the finite-amplitude baroclinic instability with this different Ekman layer friction and pointed out that the unstable wave amplitude would finally come to a non-zero equilibrium along with the different friction between the upper and lower layers, but to a zero equilibrium without friction in the upper layer. Besides the two cases said above, this paper considers the release of convective condensation latent caused by frictional effect in the lower boundary. This kind of heating can strongly affect baroclinic instability. Having discussed the heating, Chang (1971) pointed out that the heating would bring about an increase of wave amplitude. Li (1982) pointed out that the convective condensation heating would cause the increase of baroclinic unstable growth rate and the space scale of the unstable waves to incline to the short-wave range. Lu (1984) also pointed out that convective heating is a main source of energy causing the amplifying baroclinic disturbance and it is not only the driving mechanics of the development of disturbance, but also provides the effective potential energy much more than the energy coming from the basic flow for the disturbances to develop, thus making the baroclinic disturbances develop rapidly. However, the results of this paper reveal that the multiple equilibrium of baroclinic instability wave amplitude can be converted into a single equilibrium as the intensity of convective heating exceeds a certain limit.

II. MODEL AND RESULTS OF LINEAR ANALYSIS

The large-scale dynamic problem in the middle and high latitudes can be discussed by using the assumption of quasi-geostrophic theory. Therefore, in the model, we adopt the dimensionless quasi-geostrophic vorticity equation and thermodynamic equation as follows:

$$\frac{d^{(0)}}{dt}(\zeta^{(0)}+\beta y)=\frac{1}{\rho_s}\frac{\partial}{\partial z}(\rho_s w^{(1)}), \tag{1}$$

$$\frac{d^{(0)}}{dt}\theta^{(0)}+\bar{S}w^{(1)}=H, \tag{2}$$

where the superscripts "0" and "1" denote zero order and one order of variable, respectively. For example, for vorticity ζ, we have

$$\zeta=\zeta^{(0)}+\varepsilon\zeta^{(1)}+\cdots,$$

where ε is Rossby number, H is heating rate, $\bar{S}$ is constant static stability parameter, and the rest are normal marks. For a complete derivation of time, we take

$$\frac{d^{(0)}}{dt}=\frac{\partial}{\partial t}+u^{(0)}\frac{\partial}{\partial x}+v^{(0)}\frac{\partial}{\partial y}.$$

We divide the atmosphere into two layers. The thickness of the upper layer and that of the lower layer are D_1 and D_2, respectively. The total thickness is D, as is shown in Fig. 1. Then, Eq. (1) is written in the first and second layers, and Eq. (2) is written in the middle layer (M). Besides, take the upper and lower boundary conditions as follows

$$w^{(1)}(z_T)=-\frac{E_{vT}^{1/2}}{2\varepsilon}\zeta^{(0)}(x,y,z_1),$$

$$w^{(1)}(z_B)=-\frac{E_{vB}^{1/2}}{2\varepsilon}\zeta^{(0)}(x,y,z_2),$$

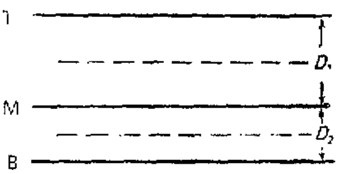

Fig. 1. The two-layer model.

where the subscripts denote the values in the corresponding layer. $F_r=f^2L^2/gD$ is Froude number, $E_v=2A_v/fD$ is the vertical Ekman number and L is characteristic length. Thus, we can obtain

$$\left[\frac{\partial}{\partial t}+\frac{\partial\psi_1}{\partial x}\frac{\partial}{\partial y}-\frac{\partial\psi_1}{\partial y}\frac{\partial}{\partial x}\right][\nabla^2\psi_1-F(\psi_1-\psi_2)+\beta y]=-r_1\nabla^2\psi_1-H(z_M)/S, \tag{3}$$

$$\left[\frac{\partial}{\partial t}+\frac{\partial\psi_2}{\partial x}\frac{\partial}{\partial y}-\frac{\partial\psi_2}{\partial y}\frac{\partial}{\partial x}\right][\nabla^2\psi_2+F(\psi_1-\psi_2)+\beta y]=-r_2\nabla^2\psi_2+H(z_M)/S, \qquad (4)$$

where $D_1\rho_s(z_1)=D_2\rho_s(z_2)$ is assumed, and

$$S=\frac{\rho_s(z_2)D_2/D}{\rho_s(z_1)D_1/D}\tilde{S}(z_M),$$

$$r_1=\frac{\rho_s(z_T)}{\rho_s(z_1)D_1/D}\frac{E_{VT}^{1/2}}{2\varepsilon},$$

$$r_2=\frac{\rho_s(z_B)}{\rho_s(z_2)D_2/D}\frac{E_{VB}^{1/2}}{2\varepsilon},$$

$$F=\frac{\rho_s(z_M)F_r\theta_s(z_M)}{\rho_s(z_1)[\theta_s(z_1)-\theta_s(z_2)]D_1/D},$$

$$\psi_1=p^{(0)} \text{ and } u^{(0)}=-\partial\psi/\partial y,\ v^{(0)}=\partial\psi/\partial x.$$

For H term on the right of Eq. (4), we only consider the heating of convective condensation and use the following linear program:

$$H(z_M)=\tilde{m}w^{(1)}(z_B),$$

where $\tilde{m}$ is a proportional constant.

Now, we consider

$$\psi_n=\bar{\Psi}_n(y)+\phi_n(x,y,t),\quad n=1,2,$$

where $\bar{\Psi}_n(y)$ is the basic stream function and it possesses such a relationship to the corresponding pure zonal flow,

$$U_n(y)=-\partial\bar{\Psi}_n/\partial y,\quad n=1,2,$$

where $\phi_n(x,y,t)$ is the disturbance function. For the time being, in this model barotropic instability caused by the horizontal shear is not included, that is, U_n has no relation to y, but $U_1\neq U_2$ because of the baroclinic state. Thus, Eqs. (3) and (4) can be written as follows:

$$\left(\frac{\partial}{\partial t}+U_1\frac{\partial}{\partial x}\right)q_1+\frac{\partial\phi_1}{\partial x}(\beta+FU_s)+J(\phi_1,q_1)+r_1\nabla^2\phi_1+m^*r_2\nabla^2\phi_2=0, \qquad (5)$$

$$\left(\frac{\partial}{\partial t}+U_2\frac{\partial}{\partial x}\right)q_2+\frac{\partial\phi_2}{\partial x}(\beta-FU_s)+J(\phi_2,q_2)+r_2\nabla^2\phi_2-m^*r_2\nabla^2\phi_2=0, \qquad (6)$$

where

$$q_n=\nabla^2\phi_n+(-1)^nF(\phi_1-\phi_2),\quad n=1,2,$$

$$U_s=U_1-U_2$$

$$J(\phi_n,q_n)=\frac{\partial\phi_n}{\partial x}\frac{\partial q_n}{\partial y}-\frac{\partial\phi_n}{\partial y}\frac{\partial q_n}{\partial x},\ n=1,2,$$

$$m^*=\tilde{m}/S.$$

The boundary conditions corresponding to (5) and (6) are

$$\frac{\partial\phi_n}{\partial x}=0 \text{ and } \frac{\partial^2\bar{\phi}_n}{\partial t\partial y}=0,\ n=1,2,\ \text{at } y=0,1, \qquad (7)$$

where $\bar{\phi}_n$ is the average value of ϕ_n in x direction.

When the variable disturbance is smaller than that of basic flow, Eqs. (5) and (6) are then linearized, and the form of the solution is

$$\begin{bmatrix}\phi_1\\ \phi_2\end{bmatrix}=\begin{bmatrix}A_1\\ A_2\end{bmatrix}\frac{1}{2}e^{i\theta}\sin ly+(*), \tag{8}$$

where $\theta=k(x-ct)$, $l=n\pi$, $n=1,2,\cdots$; the asterisk (*) represents the complex conjugate of the preceeding expression. Thus, the resulting eigenvalue yields the following equation for c:

$$c=\frac{U_1+U_2}{2}-\frac{-2\beta(a^2+F)+a^2Z/ik+\sqrt{X+iY}}{2a^2(a^2+2F)}, \tag{9}$$

where

$$a^2=k^2+l^2,$$
$$Z=(a^2+F)[r_1+r_2(1-m^*)]+Fm^*r_2,$$
$$X=U_s^2a^4(a^4-4F^2)+4\beta^2F^2-[Z^2-4a^2(a^2+2F)(1-m^*)r_1r_2](a^2/k)^2,$$
$$Y=4\beta\{F^2[r_1-r_2(1-m^*)]+(a^2+F)Fm^*r_2\}(a^2/k)$$
$$-2a^2(a^2+2F)U_s\{(a^2-F)[r_1-r_2(1-m^*)+Fm^*r_2]\}(a^2/k).$$

Therefore, considering various parameter, such as a, β, r_1, r_2, m^* and so on, we can analyse their effects on the linear baroclinic instability. Under the frictionless condition ($r_1=r_2=0$), Pedlosky (1970) already discussed this, which will not be repeated here.

In the case of friction, that is, the frictional coefficient r_1 and r_2 are not zero at the same time. The imaginary part of Eq. (9) taking zero yields the marginal shear. Now we discuss the various parameters, such as β-effect, friction and convective heating, respectively. And in the calculation we take $F=14$, $\beta=3.508$, $l=\pi$. The heating intensity $m^*=1$ is about 1°C per day in actual atmosphere. In the figures, we have $A^{*2}=a^2/F$, $l^{*2}=l^2/F$, $U_c^*=U_cF$.

Figures 2 and 3 show the effect of friction and convective heating on the stability in the case of no β-effect. And the curves of positive and negative marginal shear corresponding to the wave number axis are symmetric. The figures show that the friction plays a role in stabilization while the heating in destabilization. Besides, it is clear that there exist long wave cutoff and short wave cutoff in the case of $r_1=r_2$ with $m^*<1$, or $r_1\neq r_2$ with weaker heating (m^* is smaller), respectively. But in the case of $r_1\neq r_2$ with stronger heating ($m^*\to 1$), the short wave cutoff goes to infinite. This shows that the unstable region extends to short wave as convective heating increases.

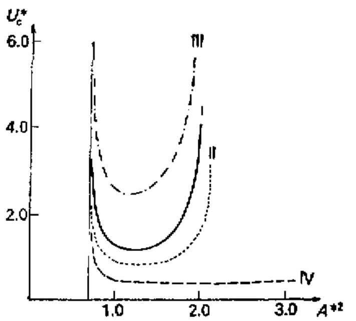

Fig. 2. $\beta=0$, I: $r_1=r_2=0.1$, $m^*=0.1$;
II: $r_1=r_2=0.1$, $m^*=0.5$;
III: $r_1=r_2=0.2$, $m^*=0.1$;
IV: $r_1=r_2=0.2$, $m^*=0.92$.

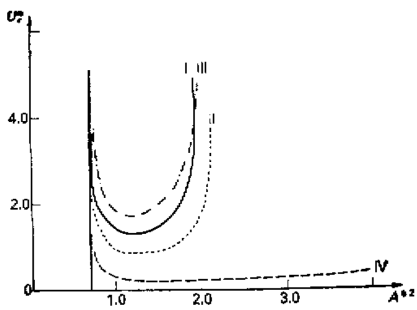

Fig. 3. $\beta=0$, I: $r_1=0.1$, $r_2=0.11$, $m^*=0.1$;
II: $r_1=0.1$, $r_2=0.11$, $m^*=0.5$;
III: $r_1=0.1$, $r_2=0.2$, $m^*=0.1$;
IV: $r_1=0.1$, $r_2=0.2$, $m^*=0.92$.

In the condition that there exists β-effect, Romea (1977) pointed out that the curves of positive and negative marginal shear corresponding to the wave number axis are symmetric if the coefficients of the upper and lower friction are equal to non-heating. But in the case of $r_1 \neq r_2$, it is shown in Fig. 4 that the combination β-effect with the frictional coefficients of the unequal upper and lower layer can make the curves of marginal shear lose symmetry although there is no heating. And the asymmetry of the curves in Fig. 4 makes the positive shear be more unstable than the negative shear with the same absolute value. Figures 5 and 6 are the cases in which the heating effect is considered. The interaction of β-effect with the heating can also change the symmetry of the positive and negative marginal curves. For the curves II in Fig. 5, it must be especially pointed out that the positive marginal shear curve is cut off at the wave number (A_σ^{*2}) as the wave number A^{*2} increases, and is called medium wave cutoff. In this case, a curve appearing on the lower half plane goes together with the U_c^*- curve and is then cut off at the wave number A_α^{*2} (A_α^{*2} is the short wave cutoff). The unstable region

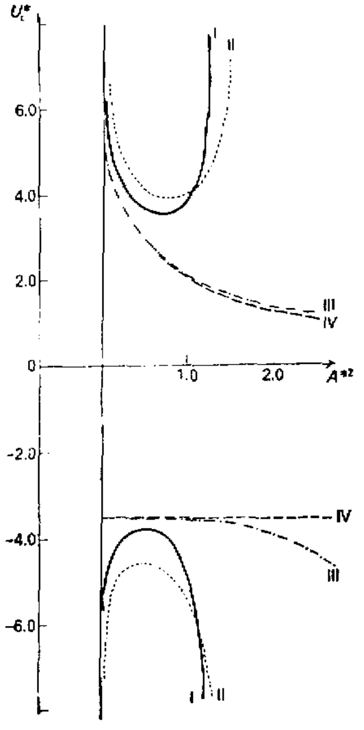

Fig. 4. $\beta=3.508$, $m^*=0$;
I: $r_1=0.1$, $r_2=0.2$;
II: $r_1=0.1$, $r_2=0.5$;
III: $r_1=0.001$, $r_2=0.1$;
IV: $r_1=0$, $r_2=0.1$.

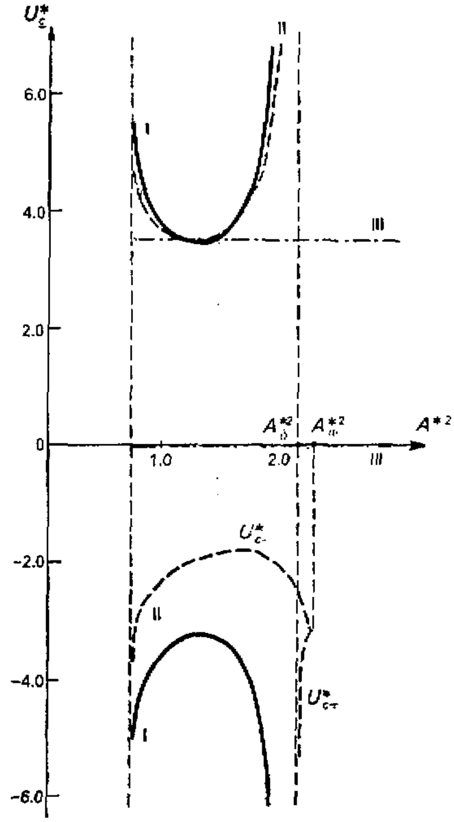

Fig. 5. $\beta=3.508$, $r_1=r_2=0.1$.
I: $m^*=0.1$;
II: $m^*=0.5$;
III: $m^*=1.0$.

on the upper half plane is above the U_c^*+ curve, but on the lower half plane is below the area surrounded by U_c^*- curve and the branching U_c^*+ curve. This branching can also be seen in Fig. 4 as well as in curve II. Because their branching phenomena are not very clear in these figures, they are not given. From Fig. 6 in the case of $r_1 \neq r_2$ it is shown that the U_c^*- curve can appear on the upper half plane for stronger heating. This indicates that it is always unstable not only for negative shear but also for weak positive shear, and it is also unstable for proper positive shear. The stable region is only between the U_c^*+ curve and the U_c^*- curve.

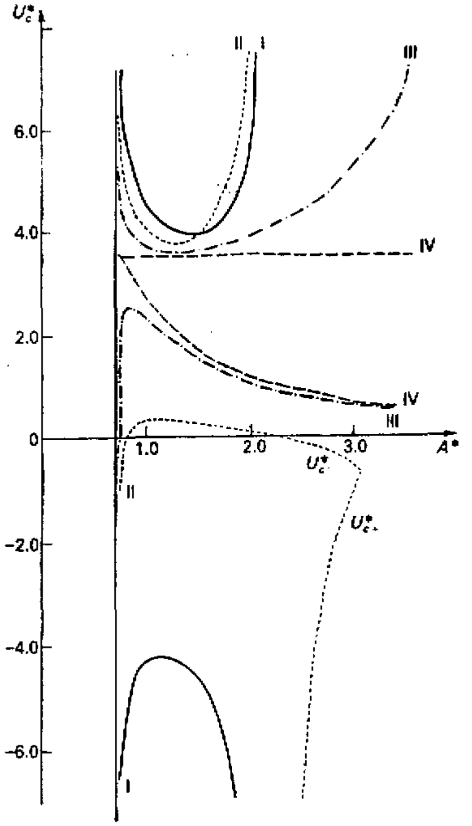

Fig. 6. $\beta=3.508$, $r_1=0.1$, $r_2=0.5$.
I: $m^*=1.0$; II: $m^*=0.7$;
III: $m^*=0.92$; IV: $m^*=1.0$.

In the case of heating $m^*>1$, the baroclinic instability appears more easily. From the basic equations of (5) and (6), it is shown that if $m^*>1$, the term of the friction (r) will be cancelled out by the heating (m^*), then turned into "negative friction" at the lower layer, i.e. in (6). At the upper layer, i.e. in (5), the proportion of the two terms is

$$r_1\nabla^2\phi_1/m^*r_2\nabla^2\phi_2=r_1A_1/m^*r_2A_2,$$

which is related to the amplitude proportion of the upper layer and lower layer (A_1/A_2).

Substitution of the wave solution formula (8) into the linear Eqs. (5) and (6) yields

$$\frac{A_1}{A_2}=\frac{a^2+F}{F}+\frac{\beta-FU_s+ir_2(1-m^*)a^2/k}{F(c-U_2)}.$$

Therefore, there is the case of "negative friction" at the upper layer, i.e. in Eq. (5), and it is almost always baroclinically unstable for any shear U_s^*, when A_1 and A_2 take proper module and phase margin. Figure 7 is the case of the marginal shear for $m^*>1$. The region surrounded by this curve is a stable one. It is obvious that the bigger (m^*-1), the smaller the stable region.

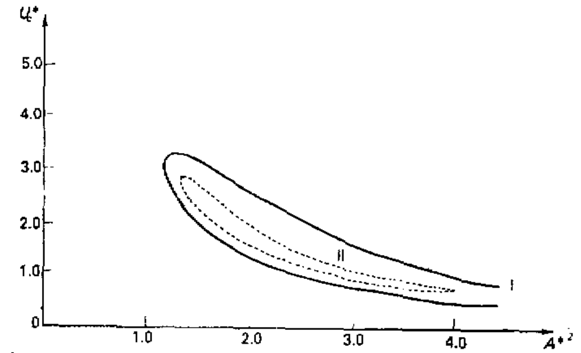

Fig. 7. $\beta=3.508$, $r_1=0.1$, $r_2=0.5$.
I: $m^*=1.2$; II: $m^*=1.4$.

III. THE NONLINEAR APPROXIMATION SOLUTION AND THE RESULTS OF NUMERICAL CALCULATION

By use of multiple time scale method, the instability problem of weak nonlinear finite amplitude near the marginal shear can be examined. Equations (5) and (6) can be rewritten as follows:

$$\left(\frac{\partial}{\partial t_*}+U_1\frac{\partial}{\partial x}\right)q_1+\frac{\partial\phi_1}{\partial x}(\beta+FU_s)=-\epsilon J(\phi_1,q_1)-r_1\nabla^2\phi_1-m^*r_2\nabla^2\phi_2, \quad (10)$$

$$\left(\frac{\partial}{\partial t_*}+U_2\frac{\partial}{\partial x}\right)q_2+\frac{\partial\phi_2}{\partial x}(\beta-FU_s)=-\epsilon J(\phi_2,q_2)-r_2\nabla^2\phi_2+m^*r_2\nabla^2\phi_2, \quad (11)$$

where t is rewritten as t_*, and ϵ is a measure of the amplitude of the disturbance relative to the basic state. The shear U_s is represented by $U_s=U_c+\Delta$, where $\Delta\ll U_c$. U_c and Δ are the marginal shear and the deviation, respectively. The highest order of the frictional coefficient r_1 and r_2 is supposed to be $O(\Delta)$, and then three time scales are introduced as follows:

$$t=t_*,\quad T=\Delta^{1/2}t_*,\quad \tau=\mu t_*,$$

where the slowly varying small parameter $\mu=O(r_2)$. So the time derivative can be written as

$$\frac{\partial}{\partial t_*}=\frac{\partial}{\partial t}+\Delta^{1/2}\frac{\partial}{\partial T}+\mu\frac{\partial}{\partial\tau}.$$

Substitute these expressions into (10) and (11), add them up, and take one from the other, then we have

$$\mathscr{L}_1(\phi_B,\phi_T) = -\Delta^{1/2}\frac{\partial q_B}{\partial T} - \mu\frac{\partial q_B}{\partial \tau} - \frac{\Delta}{2}\frac{\partial}{\partial x}(q_B+q_T) - F\Delta\frac{\partial \phi_T}{\partial x} - \epsilon J(\phi_B,q_B)$$

$$-\epsilon J(\phi_T,q_T) - \frac{r_1-r_2}{2}\nabla^2\phi_B - \frac{r_1-r_2}{2}\nabla^2\phi_T. \tag{12}$$

$$\mathscr{L}_2(\phi_B,\phi_T) = -\Delta^{1/2}\frac{\partial q_T}{\partial T} - \mu\frac{\partial q_T}{\partial \tau} - \frac{\Delta}{2}\frac{\partial}{\partial x}(q_T-q_B) - F\Delta\frac{\partial \phi_B}{\partial x} - \epsilon J(\phi_B,q_T)$$

$$-\epsilon J(\phi_T,q_B) - \frac{r_1+r_2}{2}\nabla^2\phi_T - \frac{r_1-r_2}{2}\nabla^2\phi_B - m^* r_2\nabla^2(\phi_B-\phi_T). \tag{13}$$

The symbols in the equations are shown in Appendix I. The boundary conditions corresponding to Eqs. (12) and (13) are

$$\frac{\partial \phi_B}{\partial x}=0,\quad \frac{\partial \phi_T}{\partial x}=0,\quad at\quad y=0,1, \tag{14a}$$

$$\frac{\partial^2 \overline{\phi}_B}{\partial t\partial y}=0,\quad \frac{\partial^2 \overline{\phi}_T}{\partial t\partial y}=0,\quad at\quad y=0,1. \tag{14b}$$

For convenience, we suppose $\epsilon\sim O(\Delta^{1/2})$, thus having

$$O(\mu)\sim O(\epsilon^2)\sim O(r_1)\sim O(r_2).$$

Both ϕ_B and ϕ_T are expanded in terms of

$$\begin{bmatrix}\phi_B\\ \phi_T\end{bmatrix}=\begin{bmatrix}\phi_B^{(1)}\\ \phi_T^{(1)}\end{bmatrix}+\epsilon\begin{bmatrix}\phi_B^{(2)}\\ \phi_T^{(2)}\end{bmatrix}+\epsilon^2\begin{bmatrix}\phi_B^{(3)}\\ \phi_T^{(3)}\end{bmatrix}+\cdots. \tag{15}$$

Substitution of the expansions into Eqs. (12) and (13) can yield the expressions of each expansion coefficient. The approximation for $O(\epsilon^0)$ is

$$\mathscr{L}_1(\phi_B^{(1)},\ \phi_T^{(1)})=0,\quad \mathscr{L}_2(\phi_B^{(1)}\phi_T^{(1)})=0. \tag{16a,b}$$

Substitution of the wave solution like (8) into (16a) and (16b) yields

$$c=U-U_c/2-\beta(a^2+F)/a^2(a^2+2F), \tag{17}$$

$$\frac{A_T^{(1)}}{A_B^{(1)}}=\gamma\equiv\frac{\beta+[c-(U-U_c/2)]a^2}{a^2U_c/2}=-\frac{FU_c-a^2U_c/2}{\beta+[C-(U+U_c/2)](a^2+2F)}, \tag{18}$$

where $U=U_c$. This is the neutral solution where there are no friction and convective heating. Take

$$A_B^{(1)}=A(T,\tau),\quad \text{thus}\quad A_T^{(1)}=\gamma A(T,\tau).$$

The approximation at $O(\epsilon^0)$ can only yield the relative proportion γ of the baroclinic disturbance amplitude A_T to the barotropic disturbance amplitude A_B. In order to determine the specific disturbance amplitude, the approximation of higher order must further be examined.

Approximations of $O(\epsilon)$, $O(\epsilon^2)$ and $O(\epsilon^3)$ of Eqs. (12) and (13) can be obtained using Pedlosky's method (1983). Substitution of the wave solution into their approximations and introduction of zonal flow corrections $\Phi_B^{(i)}(y,T,\tau)$ and $\Phi_T^{(i)}(y,T,\tau)(i=2,3)$ produced by nonlinear effect in the approximations of $O(\epsilon)$ and $O(\epsilon^2)$ yield the approximate equations of each order by eliminating the secular terms. Then these equations are recombined and called the reconstituted equations. Because neither $\Phi_B^{(i)},\Phi_T^{(i)}$ nor A are functions of fast time scale, the time derivative can be rewritten as

$$\frac{\partial}{\partial t_*}=\Delta^{1/2}\frac{\partial}{\partial T}+\mu\frac{\partial}{\partial \tau} \quad \text{and} \quad \frac{\partial^2}{\partial t_*^2}=\Delta\frac{\partial^2}{\partial T^2}+2\Delta^{1/2}\mu\frac{\partial^2}{\partial T\partial \tau}+O(\epsilon^4).$$

Take

$$\Phi_B=\Phi_B^{(2)}+\epsilon\Phi_B^{(3)}+O(\epsilon^2),$$
$$\Phi_T=\Phi_T^{(2)}+\epsilon\Phi_T^{(3)}+O(\epsilon^2),$$

and let

$$\begin{cases} t=\sigma t_*, \\ \sigma=k[\Delta U_c(2F-a^2)/2(2F+a^2)]^{1/2}, \\ \Phi_B=(Fl\epsilon/U_c)\Psi_B, \\ \Phi_T=(Fl\epsilon/U_c)\Psi_T, \\ \nu_n=r_n/\sigma, \quad n=1,2. \end{cases} \tag{19}$$

Thus, the reconstituted equations become

$$\frac{\partial}{\partial t}\frac{\partial^2}{\partial y^2}\Psi_B+\frac{\nu_1-\nu_2}{2}\frac{\partial^2}{\partial y^2}\Psi_B+\frac{\nu_1-\nu_2}{2}\frac{\partial^2}{\partial y^2}\Psi_T=0, \tag{20a}$$

$$\frac{\partial}{\partial t}\left(\frac{\partial^2}{\partial y^2}-2F\right)\Psi_T-\frac{\nu_1+\nu_2}{2}\frac{\partial^2}{\partial y^2}\Psi_T$$
$$+m^*\nu_2\frac{\partial^2}{\partial y^2}(\Psi_B-\Psi_T)+\frac{\nu_1-\nu_2}{2}\frac{\partial^2}{\partial y^2}\Psi_B$$
$$=\sin 2ly\{[(\nu_1+\nu_2)-\gamma(\nu_1-\nu_2)]|A|^2+d|A|^2/dt\}, \tag{20b}$$

$$\frac{d^2A}{dt^2}+(B_1+iB_2)\frac{dA}{dt}+(D_1+D_2)A=0. \tag{21}$$

The symbols in the equations are shown in Appendix II. The boundary conditions (14a) and (14b) can be rewritten as

$$\frac{\partial^2\Psi_B}{\partial t\partial y}=0 \quad \text{and} \quad \frac{\partial^2\Psi_T}{\partial t\partial y}=0 \quad \text{at } y=0,1. \tag{22}$$

From Eqs. (20a) and (20b) it is shown that the friction $(\nu_1+\nu_2)$ is always the sink of zonally averaged potential vorticity and it plays a role in damping. The term of $(\nu_1-\nu_2)$ is an exchange term between baroclinic and barotropic fields. The effect of convective heating (m^*) is opposite to that of frictional dissipation; so it is the source of the zonally averaged potential vorticity. The wave flux of potential vorticity is only related to the frictional effect and the convective heating does not contribute to it. Besides, from (20a) it is seen that if $\nu_1=\nu_2$ and initial condition is taken as $\Psi_B(y,0)=0$, Ψ_B is always zero whether there is heating effect or not. Both Ψ_B and Ψ_T are expanded in terms of cosine series

$$\begin{bmatrix}\Psi_B\\ \Psi_T\end{bmatrix}=\sum_{m=1}^{13}\begin{bmatrix}\Psi_m^{(B)}\\ \Psi_m^{(T)}\end{bmatrix}\cos(m\pi y), \tag{23}$$

where only those terms with m being odd number are non-zero ones. Assume

$$A=R(t)e^{i\phi(t)}, \tag{24}$$

where both $R(t)$ and $\phi(t)$ are real functions. Substitution of (23) into (24) and separation of the real part from the imaginary part yield

$$\frac{d^2R}{dt^2}+B_1\frac{dR}{dt}+D_1R-B_2\frac{L}{R}-\frac{L^2}{R^3}=0, \tag{25a}$$

$$\frac{dL}{dt}+B_1L=-D_2R^2-\frac{B_2}{2}\frac{dR^2}{dt}, \tag{25b}$$

where $L=R^2\frac{d\phi}{dt}$ can be considered as the "angular momentum".

In the case free of frictional effect ($\nu_1=\nu_2=0$), we obtain from (25a) and (25b)

$$\frac{d}{dt}\left\{\frac{1}{2}\left(\frac{dR}{dt}\right)^2+V(R)\right\}=0, \tag{26}$$

where

$$V(R)=\frac{1}{2}\left[\left(\frac{k\Delta}{2\sigma}\right)^2-dN^*R^2(0)-1\right]R^2+\frac{dN^*}{4}R^4+\frac{1}{2}C_0^2R^{-2},$$

$$N^*=\sum_{m=1}^{23}\left[\frac{a^2-F}{a^2}m^2\pi^2-(a^2-2F)\right]\frac{32n^2}{(m^2\pi^2+2F)(4n^2-m^2)^2\pi^2},$$

and C_0 is an integral constant which is determined by the initial value. Equation (26) indicates that the sum of kinetic energy $\frac{1}{2}(dR/dt)^2$ and potential energy $V(R)$, i.e. the total energy, is conserved in the case of frictionless condition. Therefore, in the process of the baroclinic instability the total energy has not been dissipated. The kinetic energy and potential energy can be exchanged for each other. The amplitude of disturbance fluctuates periodically.

In the case free of frictional effect on the upper layer, i.e. $\nu_1=0$, Eq. (25a) shows that there only exists a steady solution of $R_s=0$. This agrees with the result of Pedlosky (1983) obtained on the f-plane. In the case of $\nu_1\to 0$, there no longer exists a dissipative sink for the potential vorticity of the upper layer. Equation (20) shows that the potential vorticity flux of the steady wave is $\nu_2(1-\gamma)|A|^2$ and it is not zero. Therefore, the wave amplitude must vanish in the steady state in order to equilibrate between wave production and mean dissipation.

In the case where ν_1 and ν_2 are not zero and $m^*<1$, equation (25) shows that there exists non-zero steady solutions as well as a zero steady solution. In Eqs. (20a) and (20b), we take the derivative as zero and have

$$(\Psi_m^{(B)})_s=\frac{\nu_2-\nu_1}{\nu_2+\nu_1}(\Psi_m^{(T)})_s, \tag{27a}$$

$$(\Psi_m^{(T)})_s=Q_mR_s^2, \tag{27b}$$

where the expression of Q_m can be found in Appendix III. From (25b), we obtain the steady-state "angular momentum"

$$L_s=-(D_2/B_1)R_s^2. \tag{28}$$

Substituting of (27a), (27b) and (28) into (25) and taking the time derivative as zero, we have

$$R_s^2=\left[1+(D_2/B_1)^2-\frac{D_2k\Delta}{B_1\sigma}\right]\Big/\left[\left(\frac{D_2}{B_1}\right)bQ^{(1)}+dQ^{(2)}\right], \tag{29}$$

where the expressions of $Q^{(1)}$ and $Q^{(2)}$ can be found in Appendix III. It is obvious that the non-zero steady solutions of Eq. (29) are the same in absolute value but in opposite symbols.

In addition to the original zero steady solution, there are two steady solutions. This is similar to the results of Pedlosky (1981) under the circumstances of weak β effect and free from heating. He has proved that the zero solution is unstable and the other two non-zero steady solutions are stable in the case of stronger β, which equals the relative vorticity gradient. So the two non-zero steady solutions in (29) are stable (it will be confirmed in the results of the following numerical integration). It is obvious that the convective heating makes the non-zero steady solution $|R_s|$ decrease. When the heating effect increases to $m^* \geqslant 1$, Eq. (29) shows that there is no real solution, that is, there is no non-zero steady solution, but only a zero steady solution. Therefore, the heating not only makes the space scale of unstable disturbance expand to the short wave range but also makes the disturbance incline to the stable equilibrium of smaller amplitude in comparison with the case of no heating. It will be decayed to the zero amplitude equilibrium in the case of stronger heating.

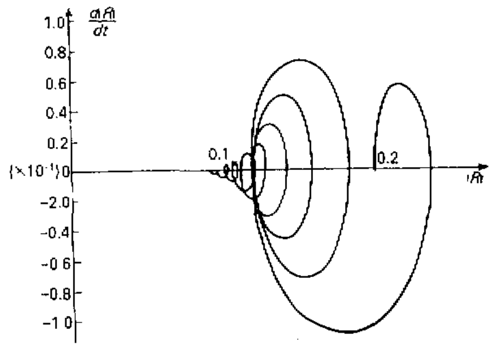

Fig. 8. $\nu_1=\nu_2=0.2$, $m^*=0.0$, $\epsilon=0.2$, $\beta=3.508$, $\Delta=0.01$, $|R_0|=0.2$.

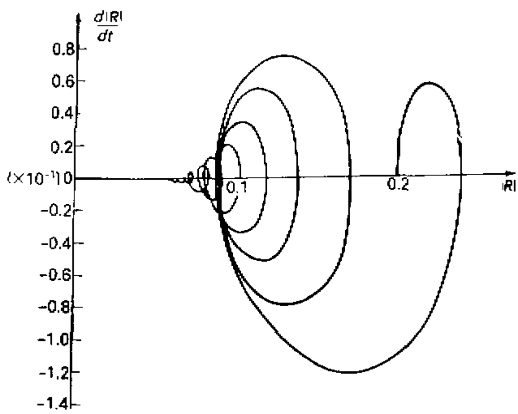

Fig. 9. $\nu_1=\nu_2=0.2$, $m^*=0.25$, $\epsilon=0.2$ $\beta=3.508$, $\Delta=0.01$, $|R_0|=0.2$,

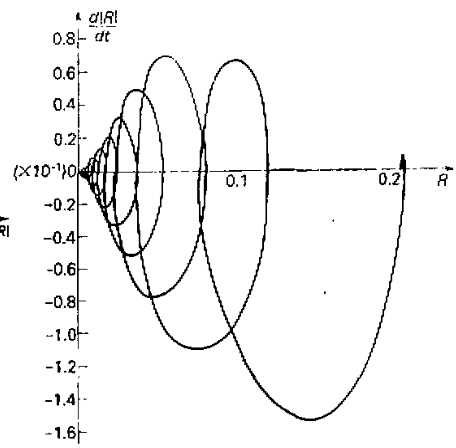

Fig. 10. $\nu_1=0.2$, $\nu_2=1.0$, $m^*=1.0$, $\epsilon=0.4$, $\beta=3.508$ $\Delta=0.01$, $|R_0|=0.2$,

By using the numerical method, Eqs. (20) and (21) are integrated, where Ψ_B and Ψ_T are substituted with expression (23). It is shown by the results that the trajectory of the solution on the phase plane of dR/dt and R wavers periodically in the case of no friction and no heating. And the trajectory decays and vacillates preiodically and inclines to the equilibrium gradually in the case of friction dissipation. Figure 8 shows the trajectory with $\nu_1=\nu_2=0.2$ and $m^*=0$. It can be seen that the curve begins to increase from the initial value ($|R_0|=0.2$) by way of linear instability. Then the wave amplitude can not increase infinitively but turns downward and decays because of the nonlinear effect. And it starts again to increase gradually when the amplitude reaches the minimum. Finally it approaches the equilibrium through the vacillation. Figure 9 is a diagram in the phase plane in the case of heating effect and the trajectory is similar to that of no heating effect, but the equilibrium $|R_s|$ decreases because of heating. In the case of $m^*\geqslant 1$, the solution inclines to the zero equilibrium, as is shown in Fig. 10, where $\nu_1=0.2$, $\nu_2=1.0$ and $m^*=1.0$.

APPENDIX I

$$\mathscr{L}_1(\phi_B,\phi_T)=\frac{\partial}{\partial t}q_B+(U-U_c/2)\frac{\partial q_B}{\partial x}+\frac{U_c}{2}\frac{\partial q_T}{\partial x}+\beta\frac{\partial\phi_B}{\partial x}+FU_c\frac{\partial\phi_T}{\partial x},$$

$$\mathscr{L}_2(\phi_B,\phi_T)=\frac{\partial}{\partial t}q_T+(U+U_c/2)\frac{\partial q_T}{\partial x}+\frac{U_c}{2}\frac{\partial q_B}{\partial x}+\beta\frac{\partial\phi_T}{\partial x}-FU_c\frac{\partial\phi_B}{\partial x},$$

$$\phi_B=(\phi_1+\phi_2)/2,\qquad \phi_T=(\phi_1-\phi_2)/2,$$

$$q_B=\nabla^2\phi_B,\qquad q_T=\nabla^2\phi_T-2F\phi_T.$$

APPENDIX II

$$B_1=[(a^2+F)(\nu_1+\nu_2)-m^*\nu_2a^2]/(a^2+2F),$$

$$B_2=k\Delta/\sigma+b\int_0^1\left[\frac{a^2+F}{a^2}\frac{\partial^2}{\partial y^2}+(a^2+2F)\right]\Psi_B\sin 2lydy,$$

$$D_1=-1+d\int_0^1\left\{-\frac{F}{a}\gamma\frac{\partial^2}{\partial y^2}\Psi_B+\left[\frac{a^2-F}{a^2}\frac{\partial^2}{\partial y^2}+(a^2-F)\right]\Psi_T\right\}\sin 2lydy,$$

$$D_2=-[-(\nu_1-\nu_2)F\gamma+(\nu_1-\nu_2)(a^2-F)+m^*\nu_2a^2(1-\gamma)]\sigma/[k\Delta(2F-a^2)],$$

$$b=4kFl\epsilon^2/[U_c\sigma(2F+a^2)],$$

$$d=4Fl\epsilon^2/[U_c\Delta(2F-a^2)].$$

APPENDIX III

$$Q_m=-\frac{8n}{(4n^2-m^2)\pi}[(\nu_1+\nu_2)+\gamma(\nu_1-\nu_2)]/\left[\frac{2(1-m^*)\nu_1\nu_2}{\nu_1+\nu_2}m^2\pi^2\right],$$

$$Q^{(1)}=\sum_{m=1}^{23}[(a^2+2F)-(1+F/a^2)m^2\pi^2]\frac{4n}{(4n^2-m^2)\pi}\cdot\frac{\nu_2-\nu_1}{\nu_2+\nu_1}Q_m,$$

$$Q^{(2)}=\sum_{m=1}^{23}\left\{\frac{F}{a^2}\gamma m^2\pi^2\frac{\nu_2-\nu_1}{\nu_2+\nu_1}+\left[(a^2-2F)-\frac{a^2-F}{a^2}m^2\pi^2\right]\right\}\frac{4n}{(4n^2-m^2)\pi}Q_m.$$

REFERENCES

Chang, C.P. (1970), On the stability of low latitude quasi-geostrophic flow in conditionally unstable atmosphere, *J. Atmos. Sci.*, **28**:270–274.

Charney, J.G. (1947), The dynamics of long waves in a baroclinic westerly current, *J. Meteor.*, **4**: 135–163.

Eady, E.T. (1949), Long waves and cyclone waves, *Tellus*, **1**:33–52.

Jaw, J.J. (1946), The formation of semipermanant centers of action in relation to the horizontal solenoid field, *J. Met.*, **3**:103–114.

Li, Chongyin (1982), On the mixed instability of long waves in atmosphere, *Science Exploration*, **2**:61–70 (in Chinese with English abstract)

Lu, Hancheng (1984), The role of cumulus convection in the development of non-geostrophic and non-linear baroclinic disturbance, *Scientia Atmospherica Sinica*, **8**:293–302 (in Chinese with English abstract)

Pedlosky, J. (1970), Finite-amplitude baroclinic waves, *J. Atmos. Sci.*, **27**:15–30.

Pedlosky, J. (1971), Finite-amplitude baroclinic waves with small dissipation. *J. Atmos. Sci.*, **28**:587–597.

Pedlosky, J. (1980), Chaotic and periodic behavior of finite-amplitude baroclinic waves, *J. Atmos. Sci.*, **37**:1177–1196.

Pedlosky, J. (1981), The effect of β on the chaotic behavior of unstable baroclinic waves, *J. Atmos. Sci.*, **38**:717–731.

Pedlosky, J. (1983), The growth and decay of finite-amplitude baroclinic waves, *J. Atmos. Sci.*, **40**:1863–1876.

Romea, R.D. (1977), The effects of friction and β on finite-amplitude baroclinic waves, *J. Atmos. Sci.*, **34**:1689–1695.